



High TNFSF13B expression as a predictor of poor prognosis in adrenocortical carcinoma

Yongxin Mao^{#^}, Parehe Alimu[#], Chenghe Wang, Wenming Ma, Ran Zhuo, Fukang Sun

Department of Urology, Ruijin Hospital, Shanghai Jiao Tong University School of Medicine, Shanghai, China

Contributions: (I) Conception and design: F Sun, Y Mao; (II) Administrative support: F Sun; (III) Provision of study materials or patients: F Sun, C Wang; (IV) Collection and assembly of data: Y Mao, P Alimu, W Ma, R Zhuo; (V) Data analysis and interpretation: Y Mao, P Alimu, W Ma, R Zhuo; (VI) Manuscript writing: All authors; (VII) Final approval of manuscript: All authors.

[#]These authors contributed equally to this work.

Correspondence to: Fukang Sun. Department of Urology, Ruijin Hospital, Shanghai Jiao Tong University School of Medicine, No. 197 Ruijin Second Road, Shanghai 200025, China. Email: sfk10570@rjh.com.cn.

Background: Adrenocortical carcinoma (ACC) is an extremely rare malignant tumor with poor prognosis. Existing treatment options have limited effects, and new therapeutic targets urgently need to be discovered. TNFSF13B has been reported to be associated with the prognosis of clear cell renal cell carcinoma, but it has not been studied in ACC.

Methods: TNFSF13B expression was analyzed and compared between ACC tumors and normal tissues by using public datasets from TCGA and GTEx. Kaplan-Meier analysis was employed to evaluate survival, and Cox regression was employed to evaluate clinicopathologic features. The upstream and downstream regulatory mechanisms of TNFSF13B were also analyzed. GSEA was performed to explore the mechanisms of TNFSF13B in ACC. Finally, 14 ACC clinical samples were used to verify the relationships between TNFSF13B expression and disease-free survival (DFS) and overall survival (OS).

Results: TNFSF13B expression was significantly higher in ACC tissues than in normal tissues. The prognosis of ACC patients with high TNFSF13B expression was worse than that of patients with low TNFSF13B expression. High TNFSF13B expression was strongly correlated with poor prognosis, and TNFSF13B was a prognostic factor. TNFSF13B expression is modified by upstream miRNAs, methylation and ubiquitination, and downstream, it interacts with other proteins. GSEA showed that regulation of cholesterol biosynthesis by SREBP and SREBF, downstream signaling events of the B cell receptor (BCR) and activation of gene expression by SREBF and SREBP were significantly enriched in the TNFSF13B high-expression phenotype. Clinical samples confirmed that TNFSF13B expression was significantly associated with DFS but not with OS.

Conclusions: TNFSF13B may be a potential prognostic molecular marker of poor survival in ACC patients, offering a new therapeutic target.

Keywords: Tumor necrosis factor ligand superfamily member 13B (TNFSF13B); adrenocortical carcinoma (ACC); prognosis

Submitted Mar 17, 2021. Accepted for publication Jun 30, 2021.

doi: [10.21037/tau-21-232](https://doi.org/10.21037/tau-21-232)

View this article at: <https://dx.doi.org/10.21037/tau-21-232>

[^] ORCID:0000-0001-7496-269X.

Introduction

Adrenocortical carcinoma (ACC) is a rare malignant tumor originating from the adrenal cortex, with an incidence rate of approximately 2.0 per million per year (1,2). The disease can occur at any age, but it has two peak ages of onset in childhood and middle age (3), and the incidence in females is slightly higher than that in males (2,4). The prognosis of the disease is extremely poor, and the overall survival (OS) time of patient is usually short (2,5-7). The complete removal of the primary tumor is one of the most important treatment methods, but local recurrence, infiltration, or distant metastasis often occur after surgery (4,8). Adjuvant therapy, such as radiotherapy or chemotherapy, has been investigated extensively in recent years. However, the exact therapeutic effect is ambiguous among multiple research teams (6,7,9-17). Mitotane is the standard treatment for patients with end-stage ACC, and it is the only drug approved by the Food and Drug Administration (FDA) and by the European Medicines Agency (EMA) for the treatment of metastatic ACC (18). The use of mitotane has a certain curative effect on the survival of patients with ACC, but the effect is limited and side effects occur (5,19-21). Therefore, new therapeutic targets urgently need to be identified. The identification of novel hub genes specific to ACC may improve the effect of targeted therapy and bring significant benefits to patients.

Tumor necrosis factor ligand superfamily member 13B (TNFSF13B), also known as BAFF, is a cytokine that belongs to the tumor necrosis factor (TNF) ligand family encoded by the TNFSF13B gene (22). This cytokine is an effective B cell activator and plays an important role in the proliferation and differentiation of B cells. It is expressed in a variety of cells, including monocytes, macrophages and dendritic cells (23,24). It is a ligand for three TNF receptors named TACI, BCMA and BAFF-R (23,25). In a bioinformatics analysis study, TNFSF13B was identified as a prognostic biomarker for renal clear cell carcinoma (26). That study concluded that high TNFSF13B expression in clear cell renal cell carcinoma leads to poor prognosis. GSEA and TIMER analyses showed that the expression of TNFSF13B was related to immune signaling pathways and lymphocyte infiltration.

However, few studies focusing on the relationship between TNFSF13B and ACC have been reported thus far, and the role of TNFSF13B in ACC remains elusive. Therefore, TNFSF13B expression was analyzed in ACC, and its expression between tumor tissues and normal tissues was compared using public datasets from The Cancer Genome Atlas (TCGA) database and the Genotype-

Tissue Expression (GTEx) project. We then analyzed the relationship between TNFSF13B expression and the clinical parameters of ACC patients and assessed the correlation of TNFSF13B expression with the disease-free survival (DFS) and OS of patients. An analysis of the upstream and downstream regulatory mechanisms of TNFSF13B was also implemented. Gene set enrichment analysis (GSEA) was performed to explore the mechanisms of TNFSF13B in ACC. Finally, we used 14 ACC clinical samples of patients recruited from Ruijin Hospital from 2013 to 2020 to verify the relationships between TNFSF13B gene expression and DFS and OS. The purpose of this study was to explore whether TNFSF13B can be used as a prognostic target in ACC patients. The significant diagnostic and prognostic value of TNFSF13B indicated that it may also be used in clinical practice to assist clinical workers in the diagnosis and treatment of ACC patients.

We present the following article in accordance with the MDAR reporting checklist (available at <https://dx.doi.org/10.21037/tau-21-232>).

Methods

Databases and identification of TNFSF13B differential expression

Gene expression profiles of ACC tissues and normal adrenal glands were downloaded from TCGA (<https://portal.gdc.cancer.gov/>) and GTEx (<https://www.gtexportal.org/home/index.html>). EdgeR (<http://bioconductor.org/>) was utilized to identify differential TNFSF13B expression between normal adrenal tissues and adrenal cortical carcinoma tissues. The difference threshold was $|\log_2FC| \geq 1$ and P value < 0.05 . The clinical data of patients, such as age, sex, pathological stage, survival and outcome, were downloaded from the TCGA database.

TNFSF13B expression and prognosis

Based on the median expression of the TNFSF13B gene, the cancer samples were divided into high and low expression groups. The correlations between the expression levels of TNFSF13B and patient DFS and OS were analyzed using the Kaplan-Meier method. Univariate Cox regression analysis was used to select possible prognostic factors.

MiRNA regulation and DNA methylation

Based on the predictions of multiple databases, the

upstream miRNA of TNFSF13B might be regulated, and the prediction results of multiple databases were analyzed by VENN. Through the miRDB, miRTarBase, miRMap, miRanda and TargetScan online prediction websites, miRNAs targeting the TNFSF13B gene were predicted, and the multiple predicted miRNAs were summarized. The miRNAs that were predicted by all five sites were considered intersecting miRNAs. We also analyzed the correlation between TNFSF13B methylation and TNFSF13B expression in ACC.

Query for E3-TNFSF13B interactions in UbiBrowser

UbiBrowser (<http://ubibrowser.ncpsb.org/>) is an integrated bioinformatics website tool designed to help users explore the predicted and reported E3 substrate interactions and ubiquitination sites of substrate proteins by querying E3 or substrate; it contains 1,295 reported E3-substrate interactions and 8,255 predicted E3-substrate interactions (27). In the network view, the central node is the substrate to be queried, and the surrounding nodes are the predicted E3 ligases. We used UbiBrowser to predict the potential E3 ligases of TNFSF13B.

Protein-protein interaction (PPI) network construction and analysis

STRING (version 11.0, <http://string-db.org>) is a database of known and predicted PPI networks (27). We used this tool to construct a PPI network and predict potential interactions between TNFSF13B and its targets. Interactions with a cutoff score of 0.4 and above were considered significant.

GSEA

GSEA software (<http://software.broadinstitute.org/gsea/downloads.jsp>) was used to identify the enrichments for biological functions and signal pathways based on the TCGA clinical data of the ACC patients. According to the expression level of TNFSF13B, the patients were divided into two groups by a median threshold: the high expression group and the low expression group. Enrichment analysis of the GSEA gene set used the C2 set (curated gene sets) in MSigDB (<http://software.broadinstitute.org/gsea/msigdb>). Finally, we sorted all enriched pathways according to the normalized enrichment score (NES).

Sample collection and quantitative real-time polymerase chain reaction (qPCR)

From 2013 to 2020, 14 ACC specimens were collected from the Department of Urology at Ruijin Hospital, Shanghai Jiao Tong University School of Medicine. The study conformed to the provisions of the Declaration of Helsinki (as revised in 2013). The institutional Committee abandoned the ethical review because it did not affect the treatment strategy. Informed consent to use their tissues for research was obtained from each patient prior to surgery. The samples were stored in liquid nitrogen. Then, total RNA was extracted by the Eastep® Super Total RNA Extraction Kit (Promega, China). A reverse-transcription kit (Promega, China) was used to reverse transcription of total RNA into the first strand of complementary DNA. QPCR was then performed with a Quantstudio™ Dx Real-Time PCR System (Thermo Fisher Scientific, USA). Endogenous gene glyceraldehyde 3-phosphate dehydrogenase (GAPDH) was used as a reference control. Genes were amplified by the following specific primers: GAPDH forward (5'-GGAGCGAGATCCCTCCAAAAT-3'), GAPDH reverse (5'-GGCTGTTGTCATACCTTCTCATGG-3'); TNFSF13B forward (5'-GGGAGCAGTCACGCCTTAC-3'), and TNFSF13B reverse (5'-GATCGGACAGAGGGGCTTT-3'). The experiment was repeated twice, and the average Ct from the values obtained for each reaction was calculated. The fold change of the target genes against that of the reference gene was calculated from the $2^{-\Delta\Delta C_t}$ values.

Statistical analysis

R 4.0.2 (<http://www.r-project.org>) and GraphPad Prism 8 (<https://www.graphpad.com>) were used for all data analyses. EdgeR was performed to explore the differential expression levels of TNFSF13B between ACC tissues and normal tissues. Kaplan-Meier survival analysis was performed to estimate the correlations between TNFSF13B expression and DFS and OS. The associations between prognosis and clinical characteristics were evaluated by univariate Cox regression analysis. The mRNA expression $2^{-\Delta\Delta C_t}$ values of clinical samples were converted logarithmically. Then, the patients were divided into a high TNFSF13B expression group and a low TNFSF13B expression group according to the median value. With the follow-up data of patients, the survival function of GraphPad Prism software was used to draw K-M survival curves. Statistical significance was

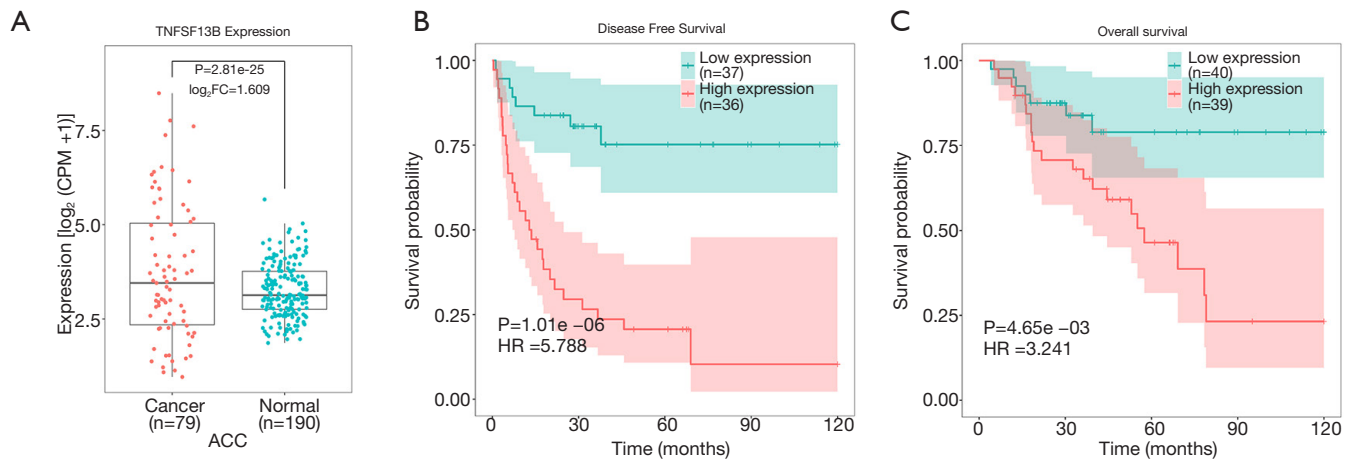


Figure 1 High expression of TNFSF13B leads to poor prognosis in ACC. (A). TNFSF13B was more highly expressed in ACC than in normal tissues. (B,C) K-M survival curves revealed that the prognosis of ACC patients with high TNFSF13B expression was worse than that of patients with low TNFSF13B expression in terms of both DFS (B) and OS (C). ACC, adrenocortical carcinoma; CPM, counts per million; DFS, disease-free survival; FC, fold change; HR, hazard ratio; OS, overall survival; TNFSF13B, tumor necrosis factor ligand superfamily member 13B.

Table 1 Univariate Cox regression analysis of the relationship between clinicopathological variables and prognosis

Clinicopathological variables	Hazard ratio	95% CI	P value
TNFSF13B expression	1.01	1–1.01	0.002
Age	1.01	0.987–1.04	0.379
Gender	1	0.469–2.14	0.999
Pathological stage	2.91	1.86–4.56	0.000
T stage	3.38	2.11–5.14	0.000
N stage	2.04	0.769–5.4	0.152
M stage	6.15	2.71–14	0.000
Tumor purity	20.3	0.148–2790	0.230
Lymph node	1.07	1.01–1.12	0.018

CI, confidence interval; TNFSF13B, tumor necrosis factor ligand superfamily member 13B.

defined as $P < 0.05$.

Results

High expression of TNFSF13B leads to poor prognosis in ACC

We compared the expression levels of TNFSF13B in 79 ACC tissues and 190 normal tissues. Table S1 lists the expression levels of TNFSF13B in a total of 269 samples. TNFSF13B was expressed at higher levels in ACC tissues than in normal adrenal gland tissues ($P < 0.0001$,

Figure 1A). Kaplan-Meier survival curves revealed that the prognosis of ACC patients with high TNFSF13B expression was worse than that of ACC patients with low TNFSF13B expression in terms of both DFS ($P < 0.0001$) and OS ($P < 0.01$) (Figure 1B,C). The univariate Cox regression analysis results showed that high TNFSF13B expression was correlated with poor prognosis [hazard ratio (HR) = 1.01, 95% confidence interval: 1–1.01, $P < 0.01$; Table 1]. Moreover, other variables, such as pathologic stage, T stage, M stage and lymph nodes, were also associated with the prognosis of ACC patients. These results indicate that the expression of TNFSF13B is a prognostic factor and

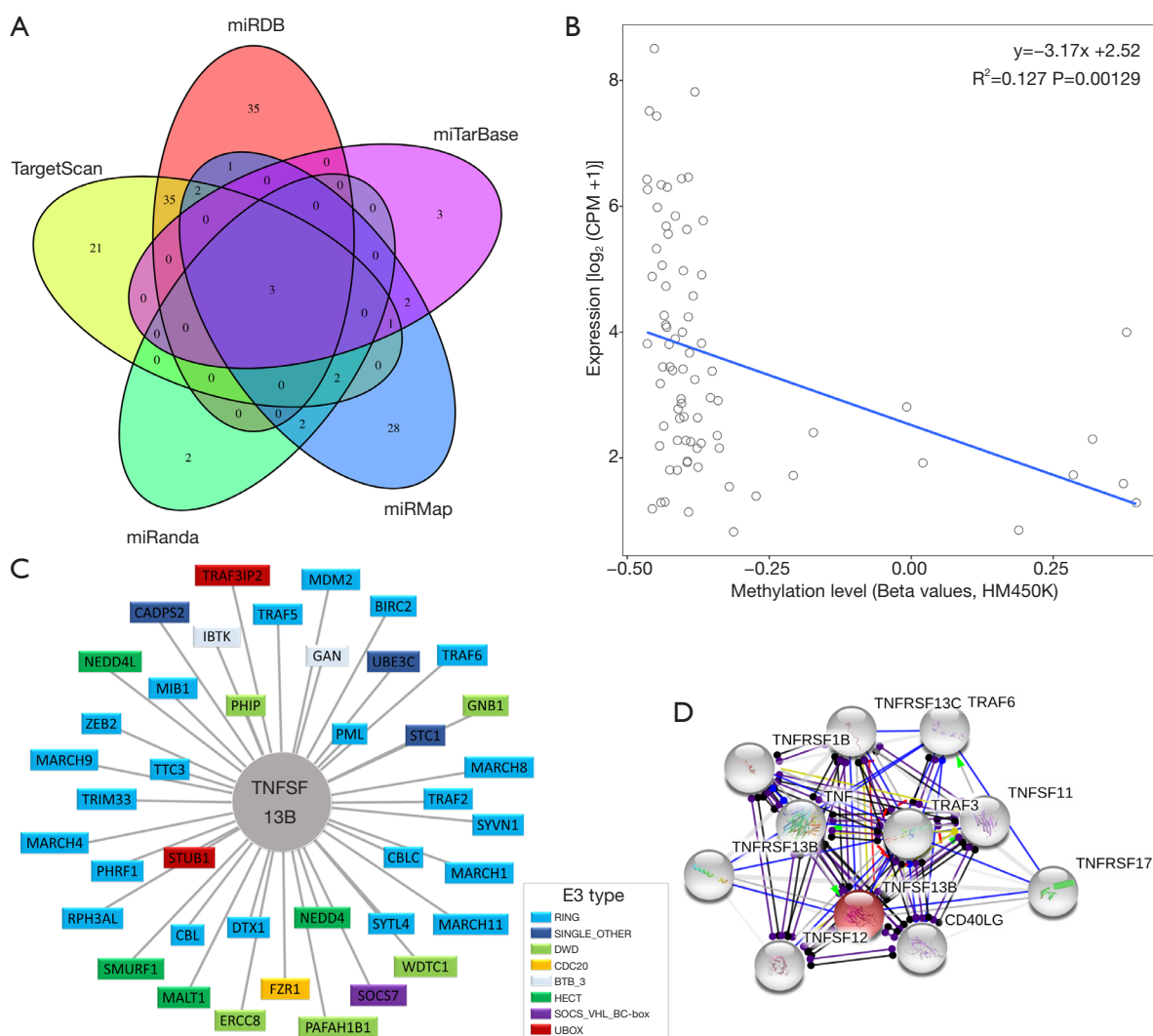


Figure 2 Upstream and downstream regulation mechanisms. (A) The miRDB, miRTarBase, miRMap, miRanda and TargetScan databases predicted 76, 9, 41, 9, and 64 miRNAs targeting TNFSF13B, respectively. The results are shown by Venn Diagram. (B) A significant negative correlation was identified between the methylation level and expression level of TNFSF13B. (C) Network view of the predicted E3-substrate interactions in the UbiBrowser web service. (D) Construction of the protein-protein interaction network between TNFSF13B and its target proteins. Abbreviations of E3 ligases are annotated in Table S2. Abbreviations of E3 type are annotated in Table S3. Abbreviations of protein-protein interaction are annotated in Table S4. CPM, counts per million; HM450K, Illumina 450k methylation arrays; TNFSF13B, tumor necrosis factor ligand superfamily member 13B.

that increased TNFSF13B levels are associated with poor DFS and OS.

Upstream and downstream regulation mechanisms

The miRDB, miRTarBase, miRMap, miRanda and TargetScan databases predicted 76, 9, 41, 9, and 64 miRNAs targeting TNFSF13B, among which there were

3 intersecting miRNAs (Figure 2A), namely, hsa-miR-30a-3p, hsa-miR-30d-3p, and hsa-miR-30e-3p. A significant negative correlation was identified between the methylation level of TNFSF13B and the expression level of TNFSF13B ($P < 0.01$) (Figure 2B). To identify the potential E3 ligases of TNFSF13B, we queried TNFSF13B as a substrate in the UbiBrowser web tool. The 4 predicted E3 ligases with middle-confidence interactions and 36 predicted E3 ligases

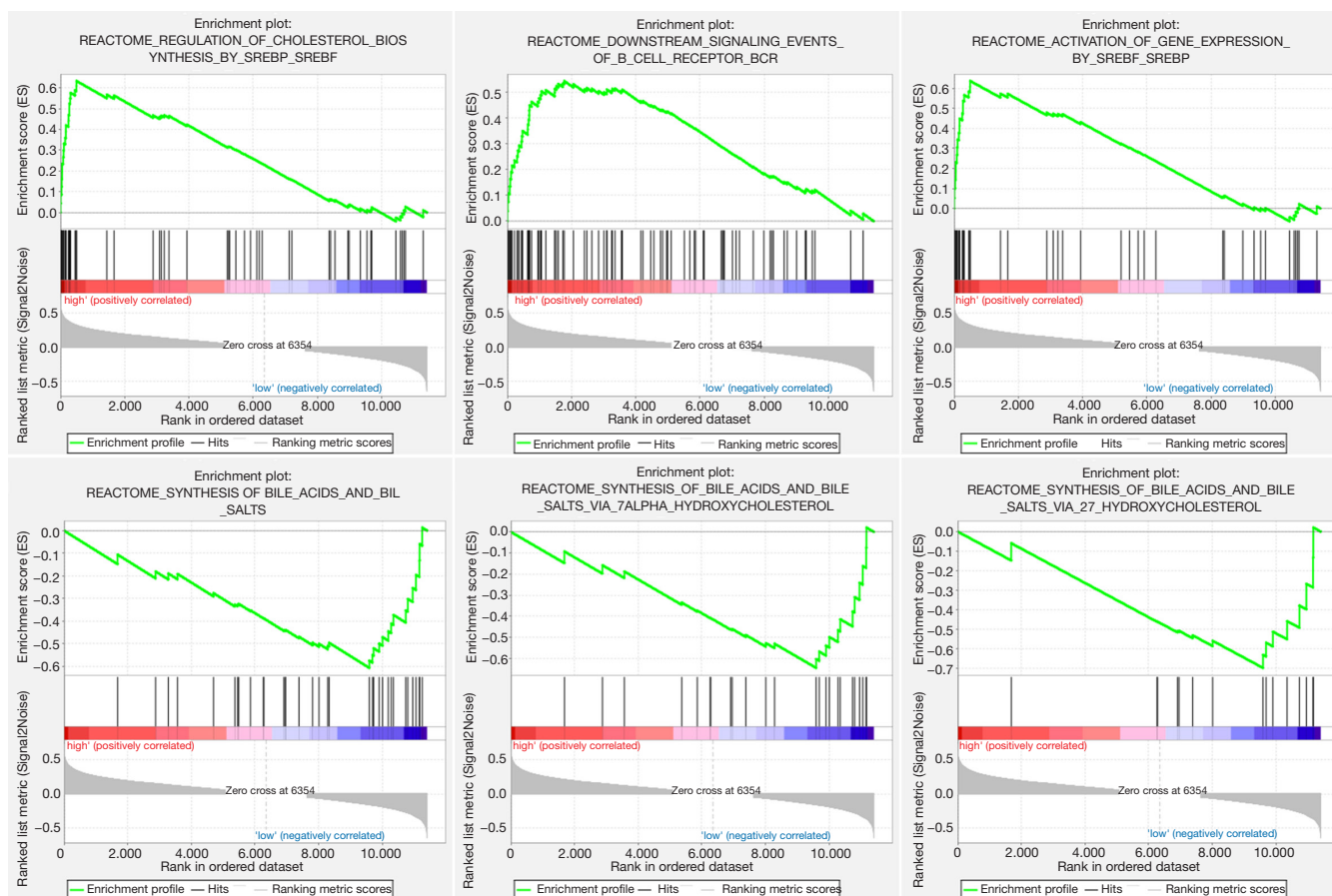


Figure 3 Gene set enrichment analysis according to the expression of TNFSF13B in TCGA. BCR, B-cell receptor; SREBF, sterol-regulatory element binding factor; SREBP, sterol-regulatory element binding protein; TCGA, The Cancer Genome Atlas; TNFSF13B, tumor necrosis factor ligand superfamily member 13B.

with low-confidence interactions are presented in [Table S2](#). *Figure 2C* displays them. The protein-protein interaction network is shown in *Figure 2D*.

GSEA

GSEA was performed to identify the potential signaling pathways involved in ACC between the low and high TNFSF13B mRNA expression groups. *Figure 3* shows the top 3 pathways in terms of the NES for the high and low TNFSF13B expression groups analyzed by GSEA. The high TNFSF13B group was enriched in the following terms: regulation of cholesterol biosynthesis by SREBP and SREBF, downstream signaling events of the B cell receptor (BCR) and activation of gene expression by SREBF and SREBP. Conversely, the low TNFSF13B group was enriched in the following pathways: synthesis of bile

acids and bile salts, synthesis of bile acids and bile salts via 7- α -hydroxycholesterol, and synthesis of bile acids and bile salts via 27-hydroxycholesterol.

Validation of clinical samples by qPCR

The ACC clinical samples of patients recruited from Ruijin Hospital were used to verify the relationship between TNFSF13B expression and prognosis. *Table 2* summarizes the demographic, clinical and pathological characteristics of the 14 patients. The scoring methods of GRAS (28) and mGRAS (29) are described in detail at the bottom of the table. As shown in *Figure 4A*, Kaplan-Meier survival curves revealed that the prognosis of ACC patients with high TNFSF13B expression was worse than that of patients with low TNFSF13B expression in terms of DFS ($P < 0.05$). However, there was no difference between the two groups

Table 2 Summary of the demographic, clinical and pathological variables of the 14 patients included in the study

Variables	n	%
Age (year)		
<50	5	35.71
≥50	9	64.29
Gender		
Male	5	35.71
Female	9	64.29
ENSAT (stage)		
I	1	7.14
II	8	57.14
III	2	14.29
IV	3	21.43
Ki67 (%)		
<10	4	28.57
10–19	4	28.57
≥20	6	42.86
GRAS [▲]		
0	4	28.57
1	3	21.43
2	4	28.57
3	3	21.43
mGRAS [▼]		
0–1	5	35.71
2–3	4	28.57
4–5	3	21.43
6–7	2	14.29
OS (months)		
≤12	3	21.43
13–24	5	35.71
>24	6	42.86
DFS (months)		
≤12	6	42.86
13–24	4	28.57
>24	4	28.57

▲The GRAS score is accumulated by the following four items (28): grade (Weiss score <3 and Ki67 <20% =0; Weiss score ≥3 or Ki67 ≥20% =1), resection status (R0 =0; R1 or R2 =1), age (<50 years =0; ≥50 years =1), and symptoms (absent =0; present =1). ▼The mGRAS score is accumulated by the following five items (29): age (<50 years =0; ≥50 years =1), symptoms (absent =0; present =1), ENSAT (stage I–II =0; stage III =1; stage IV =2), resection status (R0 =0; R1 =1; R2 =2; R3 =3), and Ki67 (0–9% =0; 10–19% =1; ≥20% =2). ENSAT, European Network for the Study of Adrenal Tumors; GRAS, Grade, Resection status, Age, and Symptoms of hormone hypersecretion; mGRAS, modified GRAS; OS, overall survival; DFS, disease-free survival.

in OS ($P=0.1413$) (Figure 4B).

Discussion

TNFSF13B is a member of the TNF superfamily. Its coding gene is located on chromosome 13q32–34 (30), and the protein it encodes is involved in many physiological activities of life. As an important B lymphocyte stimulating factor, the normal expression of TNFSF13B is important for the survival, proliferation and differentiation of B cells. TNFSF13B deficiency may lead to a decrease in humoral immune function. Studies have shown that TNFSF13B knockout mice have severe B cell defects (31), and the numbers of B cells in the splenic marginal zone and follicles are significantly reduced, which will cause a sharp drop in serum total immunoglobulin levels (32). In addition, TNFSF13B can effectively promote the apoptosis of tumor cells. TNFSF13B inhibits the growth of human lymphoma cells (U937), prostate cancer cells (PC-3), colon cancer cells (HT-29), cervical cancer cells (HeLa), breast cancer cells (MCF-7) and embryonic kidney cells (A293). In U937 cells, researchers found that TNFSF13B could induce apoptosis by activating caspase-3 to degrade PARP (33).

However, the abnormal expression of TNFSF13B is also closely related to the occurrence and development of certain diseases. First, TNFSF13B is associated with tumorigenesis. In the serum of patients with follicular-type non-Hodgkin's lymphoma, researchers found that the level of TNFSF13B was three times that in normal people (34). In another study, serum levels of TNFSF13B increased in newly diagnosed patients with IgG type multiple myeloma (MM) compared with healthy volunteers, and the concentration of TNFSF13B increased in the late stage with the progression of MM (35). In addition, TNFSF13B is believed to be related to autoimmune diseases such as rheumatoid arthritis, systemic lupus erythematosus and Sjogren's syndrome. An analysis of biological samples from patients with various autoimmune diseases confirmed that high serum TNFSF13B levels were associated with these diseases (24). Similarly, researchers found that TNFSF13B mRNA transcription levels increased in the brain tissues of experimental autoimmune encephalomyelitis mice (31). Moreover, TNFSF13B may be associated with infectious diseases. Researchers found elevated levels of TNFSF13B in the serum of HIV patients (36). Finally, TNFSF13B has important links with the occurrence and development of diabetes. Diabetes could be prevented in TNFSF13B-deficient NOD mice (37). TNFSF13B blockers inhibit the

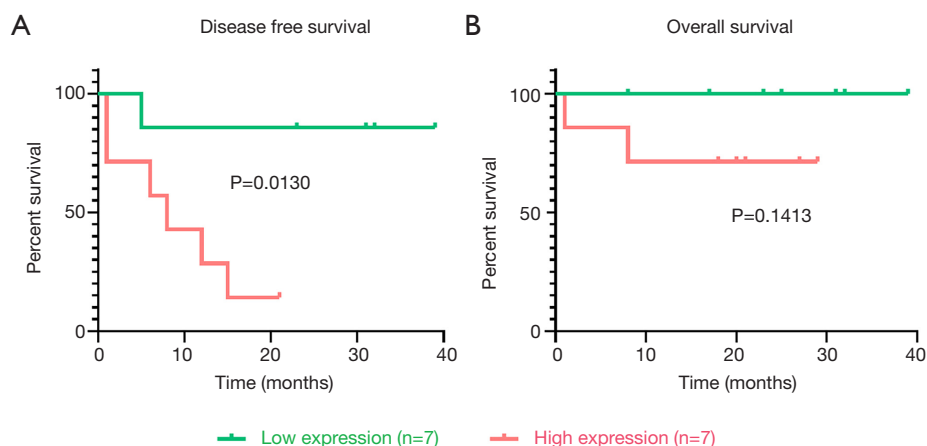


Figure 4 Relationship between the mRNA expression of TNFSF13B in ACC clinical samples and prognosis was verified by qPCR. (A). K-M survival curves revealed that the prognosis of ACC patients with high TNFSF13B expression was worse than that of patients with low TNFSF13B expression in terms of DFS. (B) K-M survival curves revealed that there was no difference between the two groups in OS. ACC, adrenocortical carcinoma; DFS, disease-free survival; OS, overall survival; qPCR, quantitative real-time polymerase chain reaction.

development of diabetes (38), and TNFSF13B-blocking compounds can delay the onset and reduce the incidence rate of diabetes (37).

At present, ACC is still a serious challenge to human medicine. Due to its low incidence, there are not as many studies on ACC as other tumors, and drugs with definite therapeutic effects are also very limited. For decades, mitotane has been the first choice of adjuvant drug for the treatment of ACC. It is recommended for people with a high risk of recurrence, and it is increasingly used as an adjuvant treatment after surgical resection of ACC. However, mitotane can affect the production of steroids (2). It can cause mitochondrial damage, interfere with the function of the mitochondrial respiratory chain, and induce the morphological fragmentation of the mitochondrial membrane necessary for the activity of the respiratory chain and the production of steroids. In addition, mitotane is a strong inducer of CYP3A4 activity, leading to the inactivation of glucocorticoids (2). Furthermore, mitotane is an inhibitor of sterol-O-acyltransferase 1 (SOAT1) (5), which causes the accumulation of free cholesterol, which is toxic to cells. However, the value of this drug is still a controversial issue, as only a few studies have compared patients in a sufficiently large treatment group with a control group (8). It is worth noting that the use of mitotane is often accompanied by some adverse reactions (5). The most common adverse reactions are neurotoxicity, such as dizziness, headache, drowsiness, and ataxia; liver damage, such as elevated transaminase; and gastrointestinal

disorders, such as nausea, vomiting, diarrhea, and upper abdominal discomfort (5). These side effects limit the use of mitotane to a certain extent.

Our study, based on public databases, found that TNFSF13B was highly expressed in ACC, and the expression level of TNFSF13B in ACC was significantly associated with poor prognosis. At the same time, we used a public database to predict factors related to the upstream and downstream mechanisms of TNFSF13B, such as miRNA regulation, methylation, ubiquitination and protein-protein interactions, which provided a direction for further study on the role of TNFSF13B in the occurrence and development of ACC. The abnormal secretion of steroid hormones, such as adrenal cortex hormones and sex hormones, is an important cause of clinical symptoms in patients with adrenal cortical cancer. Cholesterol is the precursor substance of steroid hormone synthesis (39), and its synthesis and decomposition state directly affect the metabolism of steroid hormones. The GSEA results showed that TNFSF13B is significantly related to cholesterol metabolism, which more strongly illustrates the role of TNFSF13B in the occurrence and development of adrenal cortical carcinoma. Based on this, we believe that our research is credible and clinically valuable. Our findings strongly indicate that TNFSF13B may be a potential biomarker or target of ACC, providing a potential new therapeutic target for ACC.

Although this study determined the prognostic value of TNFSF13B in ACC, there are still some limitations.

First, the number of clinical samples was too small, and the follow-up time was not long enough. For these two reasons, we failed to verify the difference in OS between the two groups. In future studies, with more cases and longer follow-up times, the important role of the TNFSF13B gene can be confirmed in ACC with poor prognosis. Second, due to the heterogeneity of the data set, there may be some errors in our analysis results. More data sets need to be used to verify our conclusions. Third, the conclusions of our analysis are based on the expression of TNFSF13B mRNA, and further research is needed to evaluate the protein expression and direct mechanism of TNFSF13B.

Conclusions

In our current study, we found that ACC patients with high TNFSF13B expression had a poorer prognosis than those with low TNFSF13B expression. TNFSF13B may be a potential prognostic molecular marker of poor survival in ACC patients, offering a new therapeutic target.

Acknowledgments

We thank the public databases for the support of this study. The public data used in this study were all downloaded in September 2020, and we cannot predict the changes that will occur afterwards. We thank WJ Xu for her help in downloading and analyzing the public data. We thank SNAS for the native language correction of this manuscript. *Funding:* This study was supported by the National Natural Science Foundation of China (81972494) and Special Research Project of Wise Healthcare of Shanghai Health and Family Planning Commission (2018ZHLY0205).

Footnote

Reporting Checklist: The authors have completed the MDAR reporting checklist. Available at <https://dx.doi.org/10.21037/tau-21-232>

Data Sharing Statement: Available at <https://dx.doi.org/10.21037/tau-21-232>

Conflicts of Interest: All authors have completed the ICMJE uniform disclosure form (available at <https://dx.doi.org/10.21037/tau-21-232>). The authors have no conflicts of interest to declare.

Ethical Statement: The authors are accountable for all aspects of the work in ensuring that questions related to the accuracy or integrity of any part of the work are appropriately investigated and resolved. The public data used in this study were all downloaded in September 2020, and we cannot predict the changes that will occur afterwards. The study conformed to the provisions of the Declaration of Helsinki (as revised in 2013). The Institutional Committee abandoned the ethical review because it did not affect the treatment strategy. Informed consent was obtained from each patient prior to surgery.

Open Access Statement: This is an Open Access article distributed in accordance with the Creative Commons Attribution-NonCommercial-NoDerivs 4.0 International License (CC BY-NC-ND 4.0), which permits the non-commercial replication and distribution of the article with the strict proviso that no changes or edits are made and the original work is properly cited (including links to both the formal publication through the relevant DOI and the license). See: <https://creativecommons.org/licenses/by-nc-nd/4.0/>.

References

1. Ettaieb M, Kerkhofs T, van Engeland M, et al. Past, Present and Future of Epigenetics in Adrenocortical Carcinoma. *Cancers (Basel)* 2020;12:1218.
2. Puglisi S, Calabrese A, Basile V, et al. New perspectives for mitotane treatment of adrenocortical carcinoma. *Best Pract Res Clin Endocrinol Metab* 2020;34:101415.
3. Pittaway JFH, Guasti L. Pathobiology and genetics of adrenocortical carcinoma. *J Mol Endocrinol* 2019;62:R105-19.
4. Berruti A, Baudin E, Gelderblom H, et al. Adrenal cancer: ESMO Clinical Practice Guidelines for diagnosis, treatment and follow-up. *Ann Oncol* 2012;23 Suppl 7:vii131-8.
5. Creemers SG, Hofland LJ, Korpershoek E, et al. Future directions in the diagnosis and medical treatment of adrenocortical carcinoma. *Endocr Relat Cancer* 2016;23:R43-69.
6. Else T, Kim AC, Sabolch A, et al. Adrenocortical carcinoma. *Endocr Rev* 2014;35:282-326.
7. Hoff AO, Berruti A. 5th International ACC Symposium: Future and Current Therapeutic Trials in Adrenocortical Carcinoma. *Horm Cancer* 2016;7:29-35.
8. Fassnacht M, Assie G, Baudin E, et al. Adrenocortical

- carcinomas and malignant pheochromocytomas: ESMO-EURACAN Clinical Practice Guidelines for diagnosis, treatment and follow-up. *Ann Oncol* 2020;31:1476-90.
9. Fassnacht M, Hahner S, Polat B, et al. Efficacy of adjuvant radiotherapy of the tumor bed on local recurrence of adrenocortical carcinoma. *J Clin Endocrinol Metab* 2006;91:4501-4.
 10. Gharzai LA, Green MD, Griffith KA, et al. Adjuvant Radiation Improves Recurrence-Free Survival and Overall Survival in Adrenocortical Carcinoma. *J Clin Endocrinol Metab* 2019;104:3743-50.
 11. Habra MA, Ejaz S, Feng L, et al. A retrospective cohort analysis of the efficacy of adjuvant radiotherapy after primary surgical resection in patients with adrenocortical carcinoma. *J Clin Endocrinol Metab* 2013;98:192-7.
 12. Hermsen IG, Groenen YE, Dercksen MW, et al. Response to radiation therapy in adrenocortical carcinoma. *J Endocrinol Invest* 2010;33:712-4.
 13. Ho J, Turkbey B, Edgerly M, et al. Role of radiotherapy in adrenocortical carcinoma. *Cancer J* 2013;19:288-94.
 14. Polat B, Fassnacht M, Pfreundner L, et al. Radiotherapy in adrenocortical carcinoma. *Cancer* 2009;115:2816-23.
 15. Sabolch A, Feng M, Griffith K, et al. Adjuvant and definitive radiotherapy for adrenocortical carcinoma. *Int J Radiat Oncol Biol Phys* 2011;80:1477-84.
 16. Al Asadi A, Hubbs DM, Sweigert PJ, et al. Analysis of adjuvant chemotherapy in patients undergoing curative-intent resection of localized adrenocortical carcinoma. *Am J Surg* 2021;222:119-25.
 17. Varghese J, Habra MA. Update on adrenocortical carcinoma management and future directions. *Curr Opin Endocrinol Diabetes Obes* 2017;24:208-14.
 18. De Filipo G, Mannelli M, Canu L. Adrenocortical carcinoma: current treatment options. *Curr Opin Oncol* 2021;33:16-22.
 19. Berruti A, Grisanti S, Pulzer A, et al. Long-Term Outcomes of Adjuvant Mitotane Therapy in Patients With Radically Resected Adrenocortical Carcinoma. *J Clin Endocrinol Metab* 2017;102:1358-65.
 20. Fassnacht M, Dekkers OM, Else T, et al. European Society of Endocrinology Clinical Practice Guidelines on the management of adrenocortical carcinoma in adults, in collaboration with the European Network for the Study of Adrenal Tumors *Eur J Endocrinol* 2018;179:G1-G46.
 21. Tang Y, Liu Z, Zou Z, et al. Benefits of Adjuvant Mitotane after Resection of Adrenocortical Carcinoma: A Systematic Review and Meta-Analysis. *Biomed Res Int* 2018;2018:9362108.
 22. Stelmach P, Pütz M, Pollmann R, et al. Alternative splicing of the TNFSF13B (BAFF) pre-mRNA and expression of the BAFFX1 isoform in human immune cells. *Gene* 2020;760:145021.
 23. Pieper K, Grimbacher B, Eibel H. B-cell biology and development. *J Allergy Clin Immunol* 2013;131:959-71.
 24. Mackay F, Ambrose C. The TNF family members BAFF and APRIL: the growing complexity. *Cytokine Growth Factor Rev* 2003;14:311-24.
 25. Kampa M, Notas G, Stathopoulos EN, et al. The TNFSF Members APRIL and BAFF and Their Receptors TACI, BCMA, and BAFFR in Oncology, With a Special Focus in Breast Cancer. *Front Oncol* 2020;10:827.
 26. Jiang M, Lin J, Xing H, et al. Microenvironment-related gene TNFSF13B predicts poor prognosis in kidney renal clear cell carcinoma. *PeerJ* 2020;8:e9453.
 27. Liu J, Han X, Chen L, et al. TRIM28 is a distinct prognostic biomarker that worsens the tumor immune microenvironment in lung adenocarcinoma. *Aging (Albany NY)* 2020;12:20308-31.
 28. Baechle JJ, Marincola Smith P, et al. Cumulative GRAS Score as a Predictor of Survival After Resection for Adrenocortical Carcinoma: Analysis From the U.S. Adrenocortical Carcinoma Database. *Ann Surg Oncol* 2021. [Epub ahead of print]. doi: 10.1245/s10434-020-09562-8.
 29. Elhassan Y, Altieri B, Berhane S, et al. Modified GRAS Score for Prognostic Classification of Adrenocortical Carcinoma: An ENSAT Multicentre Study. *J Endocr Soc* 2021;5:A165-6.
 30. Schneider P, MacKay F, Steiner V, et al. BAFF, a novel ligand of the tumor necrosis factor family, stimulates B cell growth. *J Exp Med* 1999;189:1747-56.
 31. Zhou T, Zhang J, Carter R, et al. BLyS and B cell autoimmunity. *Curr Dir Autoimmun* 2003;6:21-37.
 32. Schiemann B, Gommerman JL, Vora K, et al. An essential role for BAFF in the normal development of B cells through a BCMA-independent pathway. *Science* 2001;293:2111-4.
 33. Mukhopadhyay A, Ni J, Zhai Y, et al. Identification and characterization of a novel cytokine, THANK, a TNF homologue that activates apoptosis, nuclear factor-kappaB, and c-Jun NH2-terminal kinase. *J Biol Chem* 1999;274:15978-81.
 34. Briones J, Timmerman JM, Hilbert DM, et al. BLyS and BLyS receptor expression in non-Hodgkin's lymphoma. *Exp Hematol* 2002;30:135-41.
 35. Bolkun L, Lemancewicz D, Jablonska E, et al. BAFF and

- APRIL as TNF superfamily molecules and angiogenesis parallel progression of human multiple myeloma. *Ann Hematol* 2014;93:635-44.
36. Stohl W, Cheema GS, Briggs WS, et al. B lymphocyte stimulator protein-associated increase in circulating autoantibody levels may require CD4+ T cells: lessons from HIV-infected patients. *Clin Immunol* 2002;104:115-22.
37. Mariño E, Walters SN, Villanueva JE, et al. BAFF regulates activation of self-reactive T cells through B-cell dependent mechanisms and mediates protection in NOD mice. *Eur J Immunol* 2014;44:983-93.
38. Mariño E, Villanueva J, Walters S, et al. CD4(+)CD25(+) T-cells control autoimmunity in the absence of B-cells. *Diabetes* 2009;58:1568-77.
39. Hanukoglu I. Steroidogenic enzymes: structure, function, and role in regulation of steroid hormone biosynthesis. *J Steroid Biochem Mol Biol* 1992;43:779-804.

Cite this article as: Mao Y, Alimu P, Wang C, Ma W, Zhuo R, Sun F. High TNFSF13B expression as a predictor of poor prognosis in adrenocortical carcinoma. *Transl Androl Urol* 2021;10(8):3275-3285. doi: 10.21037/tau-21-232

Table S1 The expression levels of TNFSF13B in 79 ACC tumor tissues and 190 normal adrenal gland tissues

Group	Sample ID	TNFSF13B expression level
Cancer	TCGA.OR.A5J1.01A	35.55493254
	TCGA.OR.A5J2.01A	50.44403995
	TCGA.OR.A5J3.01A	2.49375608
	TCGA.OR.A5J5.01A	3.383237206
	TCGA.OR.A5J6.01A	0.948643688
	TCGA.OR.A5J7.01A	31.05294024
	TCGA.OR.A5J8.01A	17.29063942
	TCGA.OR.A5J9.01A	216.1420843
	TCGA.OR.A5JA.01A	7.832313437
	TCGA.OR.A5JB.01A	12.84022696
	TCGA.OR.A5JC.01A	11.28618831
	TCGA.OR.A5JD.01A	3.784010001
	TCGA.OR.A5JE.01A	62.55556935
	TCGA.OR.A5JF.01A	25.59486687
	TCGA.OR.A5JG.01A	3.800749518
	TCGA.OR.A5JI.01A	6.923947559
	TCGA.OR.A5JJ.01A	5.483135171
	TCGA.OR.A5JK.01A	12.13840993
	TCGA.OR.A5JL.01A	30.77440142
	TCGA.OR.A5JM.01A	357.5898053
	TCGA.OR.A5JO.01A	6.071012897
	TCGA.OR.A5JP.01A	91.30896983
	TCGA.OR.A5JQ.01A	5.209878186
	TCGA.OR.A5JR.01A	4.000580032
	TCGA.OR.A5JS.01A	45.24296755
	TCGA.OR.A5JT.01A	1.595162062
	TCGA.OR.A5JV.01A	16.87514915
	TCGA.OR.A5JW.01A	6.994206264
	TCGA.OR.A5JX.01A	1.737686764
	TCGA.OR.A5JY.01A	83.50195935
	TCGA.OR.A5JZ.01A	4.996911099
	TCGA.OR.A5K0.01A	69.41281441
	TCGA.OR.A5K1.01A	4.426339552
	TCGA.OR.A5K2.01A	61.25043368
	TCGA.OR.A5K3.01A	6.266915821
	TCGA.OR.A5K4.01A	1.194871844
	TCGA.OR.A5K5.01A	86.2411978
	TCGA.OR.A5K6.01A	40.6157137
	TCGA.OR.A5K8.01A	6.704437561
	TCGA.OR.A5K9.01A	194.1403784
	TCGA.OR.A5K0.01A	9.209284157
	TCGA.OR.A5KT.01A	12.87612189
	TCGA.OR.A5KU.01A	2.256451398
	TCGA.OR.A5KV.01A	79.35773497
	TCGA.OR.A5KW.01A	14.29878792
	TCGA.OR.A5KX.01A	46.89277423
	TCGA.OR.A5KY.01A	4.162913571
	TCGA.OR.A5KZ.01A	4.458480666
	TCGA.OR.A5L3.01A	34.69181656
	TCGA.OR.A5L4.01A	3.37794547
	TCGA.OR.A5L5.01A	7.795232773
	TCGA.OR.A5L6.01A	3.717030387
	TCGA.OR.A5L8.01A	1.12435183
	TCGA.OR.A5L9.01A	10.79008386
	TCGA.OR.A5LA.01A	6.985448427
	TCGA.OR.A5LB.01A	13.81257064
	TCGA.OR.A5LC.01A	60.78092724
	TCGA.OR.A5LD.01A	1.325304591
	TCGA.OR.A5LE.01A	165.0493037
	TCGA.OR.A5LG.01A	32.73825371
	TCGA.OR.A5LH.01A	17.08635199
TCGA.OR.A5LJ.01A	9.956327257	
TCGA.OR.A5LK.01A	10.21833889	
TCGA.OR.A5LL.01A	23.79068055	
TCGA.OR.A5LM.01A	12.11528084	
TCGA.OR.A5LN.01A	7.148712209	
TCGA.OR.A5LO.01A	18.63191653	
TCGA.OR.A5LP.01A	6.65272125	
TCGA.OR.A5LR.01A	1.603704285	
TCGA.OR.A5LS.01A	3.317090377	
TCGA.OR.A5LT.01A	1.862045174	
TCGA.OU.A5PI.01A	12.73407082	
TCGA.P6.A5OF.01A	69.87470928	
TCGA.P6.A5OG.01A	10.41986953	
TCGA.PA.A5YG.01A	6.224948028	
TCGA.PK.A5H8.01A	8.706739667	
TCGA.PK.A5H9.01A	1.880810031	
TCGA.PK.A5HA.01A	3.090439024	
TCGA.PK.A5HB.01A	1.897874641	
Normal	GTEX-111CU-0126-SM-5GZWW	7.136207233
	GTEX-111YS-0126-SM-5987T	13.98705725
	GTEX-1122O-0326-SM-5H124	3.500176166
	GTEX-117YX-0126-SM-5EGH5	23.10245262
	GTEX-11DXX-0126-SM-5EGH7	3.816206105
	GTEX-11DXY-1626-SM-5H12L	9.555646519
	GTEX-11DXZ-0226-SM-5EGGZ	5.927179646
	GTEX-11EM3-0326-SM-5A5KJ	27.3993174
	GTEX-11EMC-0526-SM-5EGJN	7.381548869
	GTEX-11EQ9-0126-SM-5986I	8.917507152
	GTEX-11GSP-0326-SM-5A5KW	6.753750561
	GTEX-11178-1826-SM-5A5M4	3.273735039
	GTEX-11NSD-0226-SM-5A5LR	11.28739947
	GTEX-11P7K-0126-SM-5986E	10.44931171
	GTEX-11TT1-0126-SM-5LUAA	23.2582923
	GTEX-11XUK-0126-SM-5CVLK	3.993130943
	GTEX-1211K-0126-SM-59HJE	7.831715074
	GTEX-12696-0626-SM-5EGGD	2.898698487
	GTEX-12BJ1-0526-SM-5FQUJ	12.69775796
	GTEX-12WSD-2126-SM-5LZWK	5.152994947
	GTEX-12WSG-0726-SM-5EGIG	7.561022389
	GTEX-12WSJ-0126-SM-5GCOM	10.60860315
	GTEX-12WSK-0326-SM-5GCCOJ	12.87340311
	GTEX-12WSL-0326-SM-5CVMK	14.80390007
	GTEX-12WSN-0926-SM-5GCN1	14.50774904
	GTEX-12ZZZ-0926-SM-5N9EQ	7.793649798
	GTEX-13111-0326-SM-5DUXF	5.967442508
	GTEX-131XF-0126-SM-5DUVF	7.832188729
	GTEX-131XG-1326-SM-5DUX4	5.454815694
	GTEX-131YS-2026-SM-5P9J8	7.316166283
	GTEX-132AR-1726-SM-5EGHQ	5.098840138
	GTEX-132NY-2226-SM-5J2LZ	28.46069145
	GTEX-132QS-0126-SM-5IFH9	3.587272946
	GTEX-1339X-0826-SM-5J2O6	18.78967874
	GTEX-1399R-0326-SM-5KM1X	31.7369854
	GTEX-1399S-0426-SM-5IFG5	4.854656726
	GTEX-1399U-0226-SM-5P9J2	2.906686505
	GTEX-139YR-0126-SM-5IJEY	22.04946602
	GTEX-13CF3-0126-SM-5IFFM	6.577769785
	GTEX-13D11-0426-SM-5LZYA	4.852179169
	GTEX-13FH7-0226-SM-5IFGG	4.062912862
	GTEX-13FTW-0126-SM-5IJED	4.856508235
	GTEX-13N11-0826-SM-5IJFP	5.636740873
	GTEX-13O21-0126-SM-5IJE8	8.76519904
	GTEX-13O3O-1626-SM-5KM1O	10.01699203
	GTEX-13O61-0126-SM-5KM4P	12.64613094
	GTEX-13OVI-1226-SM-5J2ME	3.792624276
	GTEX-13OW6-1726-SM-5IJJG	5.91900424
	GTEX-13OW7-2726-SM-5L3HN	7.236350891
	GTEX-13PL7-1026-SM-5MP5C	5.227765188
	GTEX-13PVR-0226-SM-5RQJI	7.277065505
	GTEX-13QBU-0526-SM-5IJFE	4.505311163
	GTEX-13W3W-1326-SM-5LUJ4T	8.765619694
	GTEX-144GL-1826-SM-79OMB	13.93482294
	GTEX-145LT-0126-SM-5S2QJ	7.658993422
	GTEX-145MN-0226-SM-5SQGPY	6.244471494
	GTEX-146FR-1526-SM-5SIB8	7.991333891
	GTEX-14753-1726-SM-5N09X	5.103283743
	GTEX-147F4-2526-SM-5NQB8	4.207814948
	GTEX-14A51-2126-SM-5NQA8	7.098095592
	GTEX-14BMU-0126-SM-5S2Q9	17.64036115
	GTEX-14C38-1726-SM-5RQJG	6.975791244
	GTEX-14C39-0226-SM-6640G	3.243797866
	GTEX-14DAQ-1826-SM-5S2VW	5.142848018
	GTEX-14DAR-1726-SM-664MZ	6.437190211
	GTEX-14E1K-0626-SM-5S2PG	4.437680727
	GTEX-14E6E-0126-SM-73KXH	5.751296316
	GTEX-14H4A-0226-SM-5SIBQ	6.060912821
	GTEX-14JG6-0126-SM-6872F	5.682021197
	GTEX-14PJ4-0426-SM-6871F	9.491477496
	GTEX-14PJ6-0126-SM-686Z5	12.68716537
	GTEX-14PK6-0126-SM-664O1	16.63675599
	GTEX-14PKV-0726-SM-686Z8	5.370617005
	GTEX-14PN3-1426-SM-686Z8	18.61439033
	GTEX-14XAO-0326-SM-6ETZN	8.953626814
	GTEX-15CHR-0626-SM-731FS	11.55137371
	GTEX-15DYW-2126-SM-6M47B	6.358482831
	GTEX-15ER7-1126-SM-6M47F	20.19352384
	GTEX-15EU6-0326-SM-6M48I	6.95501828
	GTEX-15SHU-1926-SM-7KUMO	6.435737087
	GTEX-16AAH-0226-SM-793A8	17.20732434
	GTEX-16MT8-1626-SM-7EWDW	6.795196008
	GTEX-16NGA-0126-SM-72D6U	7.599920129
	GTEX-17HGU-0126-SM-7DHLV	7.195795154
	GTEX-17HHE-0226-SM-79399	13.38114607
	GTEX-17HHY-2226-SM-7KFS4	19.51564417
	GTEX-17KH3-0326-SM-7KFS5	7.37552333
	GTEX-17KA6Q-1826-SM-72D6I	7.149256035
	GTEX-18A7A-1826-SM-7KFTU	7.098591129
	GTEX-18D9B-1926-SM-7KFSV	16.17766823
	GTEX-1A3MV-0226-SM-731FS	6.997006313
	GTEX-1A3MW-2126-SM-731DO	11.71206174
	GTEX-1AMFI-0626-SM-731DR	6.634789882
	GTEX-1AX8Z-2426-SM-72D7D	13.52344054
	GTEX-1AX9J-0626-SM-72D7L	16.49124332
	GTEX-1B8KE-0926-SM-71891	16.28810178
	GTEX-1B8KZ-0126-SM-7DHM5	8.865203916
	GTEX-1B8L1-1326-SM-7MKG6	5.809574771
	GTEX-1BAJH-2626-SM-7EPG6	7.362078725
	GTEX-1C475-0126-SM-731DC	7.71513248
	GTEX-1CAMR-0126-SM-79391	7.016725351
	GTEX-1CAMS-0226-SM-79397	5.915410997
	GTEX-1EKG2-2126-SM-7MKFT	9.666444304
	GTEX-1F5PL-2326-SM-7MKFC	14.50246939
	GTEX-1NFK9-1726-SM-3TW8P	4.119701256
	GTEX-O5Y7-1326-SM-3MJGR	49.89597857
	GTEX-O5YV-1126-SM-3LK73	9.695014773
	GTEX-OHPK-1326-SM-3MJGN	5.026055924
	GTEX-OHPL-1326-SM-3MJGG	12.85204698
	GTEX-OIZH-1326-SM-3NB1H	17.14643177
	GTEX-OQBK-3126-SM-3LK5R	10.76040306
	GTEX-OXRK-0126-SM-3NB1E	14.7827588
	GTEX-P4QS-1326-SM-3NMD3	7.146780861
	GTEX-P4QT-1326-SM-3NMD3	18.12304993
	GTEX-PLZ5-0326-SM-3P614	9.915620548
	GTEX-PLZ6-0226-SM-3P611	4.977860202
	GTEX-PW2O-0226-SM-48TC7	21.82090036
	GTEX-PWCY-0226-SM-48TD8	4.949079896
	GTEX-PXY3-1326-SM-48TU18	11.24100605
	GTEX-Q2AH-0126-SM-48U2B	9.285168898
	GTEX-Q2AI-0226-SM-48U1D	7.950354582
	GTEX-QCQG-0126-SM-48U1E	26.83504616
	GTEX-QQCG-0126-SM-48U27	10.87981443
	GTEX-QDVJ-1126-SM-48U1U	10.03900485
	GTEX-QDVN-0426-SM-48TZ6	12.7395428
	GTEX-QEG5-1826-SM-4R1JP	15.25136394
	GTEX-QLQ7-0126-SM-4R1JP	7.226845823
	GTEX-QLQW-0226-SM-447BJ	4.349725475
	GTEX-QMRM-0126-SM-4R1K9	17.24375202
GTEX-R53T-0226-SM-48FEH	6.497728691	
GTEX-R55C-0226-SM-48FEO	6.812734347	
GTEX-R55G-0126-SM-48FDS	7.707805758	
GTEX-REY6-1726-SM-48FDL	9.77919488	
GTEX-RM2N-0126-SM-48FDD	9.457509243	
GTEX-RUSQ-0226-SM-47JW1	3.5046623	
GTEX-S32W-1326-SM-4AD61	8.120357829	
GTEX-S33H-0126-SM-4AD6A	10.03798417	
GTEX-S341-0126-SM-4AD6A	7.450670499	
GTEX-S3XE-0126-SM-4AD4R	7.154484685	
GTEX-S4Q7-0226-SM-4AD5O	19.47812207	
GTEX-S4Z8-0126-SM-4GICC	8.169641869	
GTEX-T6MO-0126-SM-4DM6X	9.215719982	
GTEX-TKQ2-0226-SM-4DM6V	9.47126268	
GTEX-TMMY-0126-SM-4DXTP	4.971979082	
GTEX-U3ZM-0226-SM-4DXTA	5.270229737	
GTEX-U3ZT-0826-SM-4DXSZ	16.19983829	
GTEX-U4B1-0126-SM-4DXSN	12.44530636	
GTEX-UJMC-0226-SM-4IHLH	2.638398603	
GTEX-V1D1-0226-SM-4JBHG	7.373999971	
GTEX-V955-0126-SM-4JBH5	14.39224048	
GTEX-VJYA-0526-SM-4KL1R	4.710993087	
GTEX-VUSG-1526-SM-4KKZH	11.60007679	
GTEX-W5WG-1126-SM-4LMLK4	11.22656689	
GTEX-WFGB-0126-SM-4MLM4	22.48118354	
GTEX-WHPG-1526-SM-4M1ZK	24.2039432	
GTEX-WQUJ-0126-SM-4OQSS	16.43022178	
GTEX-WY7C-0326-SM-4OND5	5.848479615	
GTEX-WYX5-0226-SM-4QAS7	9.914502899	
GTEX-X4LF-0126-SM-4QAS7	10.45916311	
GTEX-XMK1-0226-SM-4B65D	7.893091473	
GTEX-XQ3S-1726-SM-4BOOD	13.18436255	
GTEX-XVZC-0226-SM-4BRVL	6.116539054	
GTEX-XV7Q-0226-SM-4BRV7	10.46445489	
GTEX-XYKS-0926-SM-4BRVG	16.71498566	
GTEX-Y114-0526-SM-4TT8V	3.597548235	
GTEX-Y3IK-0226-SM-51MRJ	17.14030862	
GTEX-Y5LM-0126-SM-4VBRJ	11.37076918	
GTEX-Y5V5-1326-SM-4V6G9	5.055219041	
GTEX-Y5V6-1926-SM-5IFIL	10.44559212	
GTEX-Y9LG-0126-SM-5O59W	15.31906559	
GTEX-YB5E-0226-SM-5IFIH	3.697961056	
GTEX-YF7O-0126-SM-5IFIR	3.314776163	
GTEX-YFCO-0126-SM-4W1YT	10.87499582	
GTEX-ZA64-0226-SM-5HL9C	3.421538231	
GTEX-ZDTT-0126-SM-4WKHA	3.131169427	
GTEX-ZF2S-0126-SM-4WKFO	11.34826972	
GTEX-ZLFU-0826-SM-4WWBP	7.077501019	
GTEX-ZLV1-0226-SM-4WWC1	9.735716417	
GTEX-ZLWG-0126-SM-4WWC5	3.967303771	
GTEX-ZP4G-0126-SM-4YCE3	8.713503397	
GTEX-ZT9W-0126-SM-4YCFD	4.958244359	
GTEX-ZT9X-0126-SM-4YCFD	19.28773295	
GTEX-ZTSS-0326-SM-5987M	3.706647509	
GTEX-ZUA1-1926-SM-5E45E	3.824574428	
GTEX-ZVAP-0126-SM-5NQ7D	4.214387916	
GTEX-ZVT2-0826-SM-5GIEO	7.654817797	
GTEX-ZY6K-0126-SM-5SIAM	6.465563667	
GTEX-ZYFG-0926-SM-5BC5U	8.80334943	
GTEX-ZYVF-1626-SM-5N9EH	5.751760205	
GTEX-ZZPU-1226-SM-5N9CK	5.196218151	

ACC, adrenocortical carcinoma; TNFSF13B, tumor necrosis factor ligand superfamily member 13B.

Table S2 E3 ligases predicted by Ubibrowser

Rank	E3	Description	Confidence level	Score
1	SYVN1	E3 ubiquitin-protein ligase synoviolin	MIDDLE	0.714
2	CBL	E3 ubiquitin-protein ligase CBL	MIDDLE	0.676
3	TRAF6	TNF receptor-associated factor 6	MIDDLE	0.671
4	MIB1	E3 ubiquitin-protein ligase MIB1	MIDDLE	0.668
5	MALT1	Mucosa-associated lymphoid tissue lymphoma translocation protein 1	LOW	0.657
6	TRAF3IP2	Adapter protein CIKS	LOW	0.653
7	TRAF2	TNF receptor-associated factor 2	LOW	0.653
8	TRAF5	TNF receptor-associated factor 5	LOW	0.649
9	SMURF1	E3 ubiquitin-protein ligase SMURF1	LOW	0.647
10	STUB1	E3 ubiquitin-protein ligase CHIP	LOW	0.64
11	NEDD4	E3 ubiquitin-protein ligase NEDD4	LOW	0.64
12	PAFAH1B1	Platelet-activating factor acetylhydrolase IB subunit alpha	LOW	0.64
13	MARCH1	E3 ubiquitin-protein ligase MARCH1	LOW	0.633
14	MARCH8	E3 ubiquitin-protein ligase MARCH8	LOW	0.633
15	BIRC2	Baculoviral IAP repeat-containing protein 2	LOW	0.628
16	NEDD4L	E3 ubiquitin-protein ligase NEDD4-like	LOW	0.621
17	MDM2	E3 ubiquitin-protein ligase Mdm2	LOW	0.619
18	CADPS2	Calcium-dependent secretion activator 2	LOW	0.615
19	RPH3AL	Rab effector Noc2	LOW	0.615
20	SYTL4	Synaptotagmin-like protein 4	LOW	0.615
21	WDTC1	WD and tetratricopeptide repeats protein 1	LOW	0.615
22	STC1	Stanniocalcin-1	LOW	0.615
23	IBTK	Inhibitor of Bruton tyrosine kinase	LOW	0.615
24	GNB1	Guanine nucleotide-binding protein G(l)/G(s)/G(t) subunit beta-1	LOW	0.615
25	PHIP	PH-interacting protein	LOW	0.613
26	DTX1	E3 ubiquitin-protein ligase DTX1	LOW	0.613
27	PML	Protein PML	LOW	0.613
28	CBLC	E3 ubiquitin-protein ligase CBL-C	LOW	0.613
29	PHRF1	PHD and RING finger domain-containing protein 1	LOW	0.613
30	SOCS7	Suppressor of cytokine signaling 7	LOW	0.613
31	ERCC8	DNA excision repair protein ERCC-8	LOW	0.613
32	TRIM33	E3 ubiquitin-protein ligase TRIM33	LOW	0.613
33	ZEB2	Zinc finger E-box-binding homeobox 2	LOW	0.613
34	MARCH9	E3 ubiquitin-protein ligase MARCH9	LOW	0.604
35	UBE3C	Ubiquitin-protein ligase E3C	LOW	0.604
36	FZR1	Fizzy-related protein homolog	LOW	0.604
37	GAN	Gigaxonin	LOW	0.604
38	MARCH11	E3 ubiquitin-protein ligase MARCH11	LOW	0.604
39	MARCH4	E3 ubiquitin-protein ligase MARCH4	LOW	0.604
40	TTC3	E3 ubiquitin-protein ligase TTC3	LOW	0.604

The data was queried and downloaded from UbiBrowser (<http://ubibrowser.ncpsb.org/>).

Table S3 Abbreviations of E3 type

Abbreviations	Description
BC-box	A conserved elongin BC-binding site motif
BTB	Broad-complex, tramtrack and bric à brac
CDC20	Cell division cycle protein 20
DWD	Damage specific DNA binding protein 1-binding WD40 protein
HECT	Homologous to E6-associated protein C-terminus
RING	Really interesting new gene
SOCS	Suppressors of cytokine signaling
UBOX	A modified RING motif without the full complement of Zn ²⁺ -binding ligands
VHL	Von Hippel-Lindau

Table S4 Abbreviations of protein-protein interaction

Abbreviations	Description
CD40LG	Tumor necrosis factor ligand superfamily member 5
TNF	Tumor necrosis factor
TNFRSF13B	Tumor necrosis factor receptor superfamily member 13B
TNFRSF13C	Tumor necrosis factor receptor superfamily member 13C
TNFRSF17	Tumor necrosis factor receptor superfamily member 17
TNFRSF1B	Tumor necrosis factor receptor superfamily member 1B
TNFSF11	Tumor necrosis factor ligand superfamily member 11
TNFSF12	Tumor necrosis factor ligand superfamily member 12
TNFSF13B	Tumor necrosis factor ligand superfamily member 13B
TRAF3	Tumor necrosis factor receptor associated factor 3
TRAF6	Tumor necrosis factor receptor associated factor 6